Computational Biology - Modeling of Primary Blast Effects on the Central Nervous System

David F. Moore, Antoine Jérusalem, Michelle Nyein, Ludovic Noels, Michael S. Jaffee, Raul A. Radovitzky

PII: S1053-8119(09)00143-8
DOI: doi:10.1016/j.neuroimage.2009.02.019
Reference: YNIMG 5996

To appear in: *NeuroImage*

Received date: 14 November 2008
Revised date: 2 February 2009
Accepted date: 4 February 2009

Please cite this article as: Moore, David F., Jérusalem, Antoine, Nyein, Michelle, Noels, Ludovic, Jaffee, Michael S., Radovitzky, Raul A., Computational Biology - Modeling of Primary Blast Effects on the Central Nervous System, *NeuroImage* (2009), doi:10.1016/j.neuroimage.2009.02.019

Computational Biology - Modeling of Primary Blast Effects on the Central Nervous System

David F. Moore, MD, PhD,[1] Antoine Jérusalem, PhD[2], Michelle Nyein[2], Ludovic Noels, PhD[3], Michael S. Jaffee, MD, MC, USAF, FS,[1] Raul A. Radovitzky, PhD[2]

[1]Defense and Veterans Brain Injury Center, Walter Reed Army Medical Center, Washington DC

[2]Department of Aeronautics and Astronautics, Massachusetts Institute of Technology, Cambridge, MA

[3]Aerospace and Mechanical Engineering Department, University of Liège, Liège, Belgium

Address Correspondence to:

Dr. David F. Moore, MD, PhD,
Defense and Veterans Brain Injury Center,
Walter Reed Army Medical Center,
Building 1, Room B207,
6900 Georgia Avenue NW,
Washington DC 20309-5001

Abstract

Objectives: Recent military conflicts in Iraq and Afghanistan have highlighted the wartime effect of traumatic brain injury. The reason for the prominence of TBI in these particular conflicts as opposed to others is unclear but may result from the increased survivability of blast due to improvements in body armor. In the military context blunt, ballistic and blast effects may all contribute to CNS injury, however blast in particular, has been suggested as a primary cause of military TBI. While blast effects on some biological tissues, such as the lung, are documented in term of injury thresholds, this is not the case for the CNS. We hypothesized that using bio-fidelic models, allowing for fluid-solid interaction and basic material properties available in the literature, that a blast wave would interact with CNS tissue and cause a possible concussive effect. **Methods:** The blast shockwave on CNS tissue was modeled using a coupled computational fluid-solid dynamic simulation. The model included a complex finite element mesh of the head and intra-cranial contents. The effects of threshold and 50% lethal blast lung injury were compared with concussive impact injury using the full head model allowing know upper and lower bounds of tissue injury to be applied using pulmonary injury as the reference tissue. **Results:** The effects of a 50% lethal dose blast lung injury (LD_{50}) were comparable with concussive impact injury using the DVBIC – MIT full head model. **Interpretation:** CNS blast concussive effects were found to be similar between impact mild TBI and the blast field associated with LD_{50} lung blast injury sustained without personal protective equipment. With the ubiquitous use of personal protective equipment this suggests that blast concussive effects may more readily occur in personnel due to enhanced survivability in the current conflicts.

Introduction

Military operations in Iraq and Afghanistan have brought into sharp focus military-related traumatic brain injury (TBI). Some recent reports suggest very significant numbers of Servicemembers are affected by TBI principally mild traumatic brain injury (mTBI) or concussion defined as a Glasgow Coma Scale (GCS) > 12 or loss of consciousness (LOC) < one-hour or post traumatic amnesia (PTA) < 24-hours.(Tanielian, 2008) In particular the RAND study estimates 320,000 TBIs from a total Servicemember deployment of 1.64 million (19.2% Servicemembers experiencing a probable TBI). More conservative estimates as determined from the Defense and Veterans Brain Injury Center (DVBIC) surveillance programs indicate mTBI represents ~ 10 - 20% of TBI screen positive Servicemembers. TBI is a significant civilian cause of death and morbidity in the 0 – 40 year-old range occurring typically from impact injury such motor vehicle accidents. There is a huge direct and indirect economic cost to society at large for TBI through the burden of care imposed on family members and lost earning potential. (Brazarian, 2005; Bruns, 2003)

The exposure of military personnel to the consequences of blast waves may increase the overall TBI burden. Injury from blast is defined as 1) primary blast injury directly due to the propagation of the blast wave through the tissue, 2) secondary blast injury due to tissue injury resulting from interaction with shrapnel or fragments, 3) tertiary blast injury with tissue injury due impact with environmental structures, for

example buildings or vehicle roll-over and 4) quaternary blast injury due to heat, electromagnetic pulses or toxic detonation products such as carbon monoxide. Typical military events represent a mixture of all four categories of blast tissue injury where separation or identifying the magnitude of the contributing components from primary to quaternary injury factors may be impractical. For this reason, the term Blast (+) TBI is introduced since this allows for the recognition of the concurrence of both blast and impact injury together with other blast injury mechanisms. The low frequency of primary blast CNS injury is illustrated by a recent isolated case report.(Warden et al., 2009)

No current patient-based clinical investigative evidence exists as whether blast waves 'per se' modifies or alters the underlying CNS injury cascade of TBI compared to blunt or impact injury however, given the evidence from animal studies and the parsimony of biological processes this would seem unlikely.(Petras, 1997) A blast wave is a pressure shockwave of finite amplitude resulting from an atmospheric (gas fluid) explosion releasing a large amount of energy in a short period of time. The explosive chemical energy secondary to detonation is released into thermal, electromagnetic, and kinetic energy, the latter being imparted to the surrounding material (such as soil, explosive casing, and fragments) together with the primary blast shockwave.(DePalma, 2005; Iverson, 2006; Strehlow, 1976) An idealized free-field blast is most simply described by the biphasic Friedlander waveform with a rapid rise to peak pressure and an exponential fall-off of the over pressure followed by a relatively prolonged underpressure resulting in a combination of compressive and tensile material components when the wave propagates through biological tissue.(Elsayed, 1997; Mayorga, 1997) Several

theories have been suggested to account for TBI after blast exposure such as direct propagation of the blast wave through the brain, to propagation of the pressure wave through the great vessels and secondarily to the brain, to cavitation secondary to the blast underpressure together with any associated blast electromagnetic pulses.(Moore, 2008)

Importantly it is necessary to realize that an explosion is a non-linear process characterized by a three-dimensional complex fluid flow field that may be significantly influenced by ambient and environmental boundary conditions. This may result in shock wave reflections with up to an eight-fold amplitude intensification over the primary shockwave. Such phenomenon indicates the considerable possibility for variability in military associated blast exposure and TBI resulting from a primary blast process.(Cullis, 2001; Kambouchev, 2007b)

The propagation of the shockwave within the fluid (air) and subsequent direct interaction with solid structures such as the skull and intra-cranial contents is the focus of the current paper. This allows consideration of the following hypotheses: (a) whether there is a direct interaction between a primary blast wave and CNS tissue and (b) whether such an interaction is sufficient to cause concussion or mTBI.

Recent results on fluid-structure interaction (FSI) underscore the possibility of mitigating impulse transfer from the blast wave to the structure by exploiting the FSI effect.(Kambouchev, 2006) Blast wave interaction with a material, either biological or non-biological, results in the development of waves which have longitudinal, shear (transverse), and surface (Rayleigh) wave components.(Kolsky, 1963) These waves, at

high strain-rates associated with blast, may have a differential pathological effect on the anisotropic structures of the brain, especially white matter tracts where directionality is paramount. Such a proposition is borne out by recent results using Kolsky bar or Split Hopkinson Pressure bar to generate experimentally material properties at high strain rate following the development and measurement of propagation speed of one-dimensional stress waves in solids. The bulk modulus in different tissue varied non-linearly but was effectively a monotonic function of the strain rate. The shear modulus on the other hand, although also non-linear, exhibited in some tissues more than one state across the strain rate domain.(Saraf, 2007) The strain-rate importantly, allows consideration of the Blast (+) syndrome across a continuum where lower strain-rate represent impact injury typical of motor vehicle accidents, intermediate strain-rates often those associated with ballistic injury and higher strain rates associated with blast or shock waves.(Moore, 2008)

While a lot of uncertainty exists regarding blast waves and the subsequent propagation of stress waves in the brain. Their relationship to TBI have been well studied using simulations under impact loading such as in sports or motor vehicular injuries. (Belingardi, 2005; Gilchrist, 2001; Horgan, 2004; Raul, 2006; Taylor, 2006; Zhang and Khalil, 2001; Zhang, 2004) For example, Willinger and Baumgartner, recreating motorcycle accidents, correlated Von Mises stresses (a scalar derivative function of the deviatoric component of the tissue stress tensor) with concussion and strain energy in the CSF and subdural hematoma formation. Zhang et al., recreating American football collisions, found high shear stress concentrations localized in the upper brainstem and

thalamus regions and determined that shear stress response in the upper brainstem was a good predictor for mTBI.(Willinger, 2003; Zhang, 2004)

The purpose of this paper is to develop a full head finite element model and simulate the fluid-solid interaction with a blast shockwave under open conditions. The paper will examine firstly, whether direct interaction and propagation of a detonation shockwave can occur through the skull and secondly compare these mechanical events using 'order of magnitude arguments' to other blast tissue damage such as the lung. As previously suggested a particular reason as to why TBI has been ascertained with greater frequency in the current conflicts is likely due to the significant strides in mitigation of thoracic and abdominal injury by the use of personal protective equipment (PPE). Prior to the availability of such PPE blast lung was a significant cause of military mortality and morbidity. Standardized pressure standoff (distance) curves or Bowen curves are available for a 70 kg person allowing assessment of the biological impact of blast on lung tissue. We utilized the Bowen survivability-lethality curves for unprotected pulmonary blast exposure to derive initial blast condition that could then be compared to known impact condition causing concussion.(Bass, 2006; Bowen, 1968; Stuhmiller, 1987; White, 1971)

In this way we hoped to compare significant current survivable blast injury with known impact mechanical forces causing concussion to estimate whether a concussive potential might exist from a survivable primary blast in the context of PPE use. In this work we used the Bowen curve derived threshold of lung injury of 5.2 atm and the lethal dose 50% of lung injury of 18.6 atm to consider an upper and lower bound of currently

survivable blast injury. This was then compared to impact injury typically seen to potentially cause concussion in the sports injury environment.

Methods

In order to examine and compare the effects of blast shock waves on the human head, simulations were run with a full head mesh in three different contexts: (1) a blast with overpressure of 5.2 atm or threshold lung injury, equivalent to a free air explosion of 0.0648 kg TNT at a 0.6 m standoff distance; (2) a blast with overpressure of 18.6 atm or ~ the 50% lethal dose (LD_{50}) for lung injury survival, equivalent to a free air explosion of 0.324 kg TNT at a 0.6 m standoff distance; and (3) an impact between a head traveling at 5 m/s and a stationary immovable boundary likely to result in concussive injury based on comparable impact studies in the literature.(Casson, 2008; Zhang, 2004) The overpressures for the two blast simulations were selected based on the Bowen curves, which give the estimated tolerance to a single blast at sea level for a 70-kg human oriented perpendicular to the blast.(Bowen, 1968)

Mesh Generation

High-resolution T1 MR images were downloaded from the Montreal Neurological Institute at an isotropic voxel dimension of 1 x 1 x 1 mm.(Collins, 1998) These images were merged with a bone windowed CT of head allowing skull reconstruction using a mutual information algorithm. The resulting volume set of images was then semi-automatically segmented using Amira (http://www.amiravis.com/) into topological closed regions of interest followed by export as VRML (Virtual Reality Modeling File) files.

This format was chosen because it is one of the solid model file formats accepted by the software employed for mesh generation. Amira is an imaging software analysis suite allowing structured regional labeling of image data together with filtering and co-registration. A variety of input formats and output formats are available. These VRML files were then imported into the mesh generation capabilities in the computational fluid mechanics software ICEMCFD (http://www.ansys.com/products/icemcfd.asp). This software provides a variety of meshing algorithms capable of importing CAD models of high topological and geometrical complexity with volumetric conformal computational meshes required by the blast simulations presented in this paper. In addition, the software provides mesh decimation, refinement and smoothing algorithms that can be used to optimize the mesh for computational efficiency. An unstructured finite element mesh was constructed using the Octree and Delaunay tetrahedral mesh generation algorithms. The meshes were further refined by isolation of poorly meshed areas and poorly shaped tetrahedra prior to running the computational fluid-solid dynamics code.(Deiterding, 2006)

A variety of computational meshes with different resolutions were created and it was found that meshes with fewer than 700,000 elements were too coarse to describe the intricate topology of some human head anatomical structures relevant for blast injury analysis. Among the computational models of the human head reported in the literature, the one with highest resolution model appears to be model developed by Zhang et al. comprising 314,500 elements.(Zhang, 2004) As part of the model development process, we produced several computational meshes ranging from 800,000 to 5,000,000 elements and found that coarser models did not capture either the geometric intricacies of brain

structures (e.g. gyrencephalic cortex and white matter fascicular structure) or, in turn, the mechanical fields associated with the blast wave. In order to balance mesh resolution and computational requirements, a mesh with 808,766 elements was used in the current simulations (Figure 1). The computational model differentiates 11 distinct structures characterized by mechanical properties summarized in Table 1 and 2.

Material Models and Properties

The constitutive response of brain tissue encompasses a variety of complex mechanisms including nonlinear viscoelasticity, anisotropy and strong rate dependence (strain-rate dependence).(Shen, 2005; Velardi, 2006) Several investigations have focused on characterizing this response experimentally (Coats, 2006; Gefen, 2004; LaPlaca, 2005; Miller, 2005, 2002; Morrison, 2006; Prange, 2002; Velardi, 2006) and on developing a variety of constitutive models to capture the behavior of the brain as a material.(Brands, 2004; Drapaca, 2006; Miller, 1999; Shen, 2005) Owing to the complexities and inherent variability associated with biological tissue especially the brain where marked regional variation exists, there is significant uncertainty in quantifying tissue response to material stresses particularly at high strain-rates such as those occurring with blast wave propagation. In consideration of these limitations, computational models have usually favored simpler (i.e. elastic) models with few parameters that can be quantified with less uncertainty, instead of more sophisticated models with many parameters that are harder to estimate with confidence. In the impact TBI modeling work, isotropic elastic models (where the material properties are both elastic and spatially uniform) have been used to derive the volumetric (bulk modulus) response whereas linear viscoelastic effects have

been considered in the shear or deviatoric response via a time-dependent shear modulus evolving from an instantaneous to the long-term value.(Belingardi, 2005; Willinger, 2003; Zhang and Khalil, 2001) In this context, the shear modulus is the physical parameter determining the characteristics (speed of propagation, intensity) of shear waves. These are associated with disturbances in the displacement field that are transverse to the direction of propagation of the wave. Such waves are always present in 3-dimensional wave propagation in solid materials and accompany longitudinal (pressure) wave. The material relaxation times involved are often on the order of tens to hundreds of milliseconds and higher for low deformation rates. It is thus reasonable to expect that deferred deformation or stress relaxation due to viscoelastic effects play a secondary role under blast loading, where the characteristic times seldom, if ever, exceed a few milliseconds. Therefore the linear blast stress wave properties are on a time-scale of several orders of magnitude less that where viscoelastic effects may be of significance. However, potential nonlinear viscoelastic effects may occur with relaxation times that can be much shorter at blast deformation rates, and, thus, may be relevant for the analysis. For simplicity and due to the unavailability of high-rate tissue properties, these effects were neglected in the model proposed.

For these reasons, and as a first approximation, we have adopted a simplified constitutive modeling strategy of brain material properties emphasizing effects pertinent to blast conditions. Specifically the description of the pressure wave propagating through the brain was parameterized through suitable equations of state. To this end, the volumetric response of brain tissue has been described by the Tait equation of state with

parameters adjusted to fit the bulk modulus of the various tissue types. The Tait equation allows modeling material densities over a wide range of pressure such as might occur during propagation of a blast shockwave through the brain. The deviatoric response has been described via a neo-Hookean elastic model with properties adjusted to fit reported values of the instantaneous shear modulus to allow modeling large elastic deformations as may arise under blast conditions. The Mie-Gruneiesen/Hugoniot equation of state was used to describe the volumetric response of the skull under high strain rate conditions. The constitutive properties of the tissues were determined from a literature review. Details about these constitutive models are summarized in Tables 1 and 2.

Tait and Mie-Gruneiesen Equations of State

The shock response of many solid materials is well described by the Hugoniot relation between the shock wave velocity U_s and the material velocity U_p by the simple equation form (1) below.(Drumheller, 1998; Meyers, 1994; Zel'dovich, 1967)

$$U_s = C_0 + sU_p \tag{1}$$

In this expression, C_0 and s are material parameters that can be obtained from experiments. By considering Equation (1) and conservation of mass and momentum in a control volume at the shock front, the final pressure can be calculated explicitly as a function of the Jacobian behind the shock front J_H and the reference density ahead of the shock ρ_0(Drumheller, 1998; Meyers, 1994; Zel'dovich, 1967).

$$P_H = \frac{\rho_0 C_0^2 (1 - J_H)}{[1 - s(1 - J_H)]^2} \tag{2}$$

where J_H is related to the density ρ_H, the specific volume V_H, and the deformation gradient

tensor $\mathbf{F}_H$, defined behind the shock front, by:

$$J_H = \frac{\rho_0}{\rho_H} = \frac{V_H}{V_0} = \det(F_H) \tag{3}$$

The relation Equation (2), also called the "shock Hugoniot," relates any final state of density to its corresponding pressure. The deformation path taken by the material between the initial state (P_0, V_0) and the final state (P_H, V_H) is then defined by a straight line in the (σ_1, V) plot where σ_1 is the axial stress in the shock direction: the Rayleigh line.(Drumheller, 1998; Meyers, 1994; Zel'dovich, 1967) The parameters for the Hugoniot/Mie-Gruneisen equation of state used in the simulations are given in Table 1. The values for C_0 and S are the same as those used for the skull in Taylor and Ford. (Taylor, 2006)

The Tait equation of state, which is commonly used to model fluids under large pressure variations, is given by:(Taylor, 2006)

$$p = B\left[\left(\frac{\rho}{\rho_0}\right)^{\Gamma_0+1} - 1\right] \tag{4}$$

Where B and Γ_0 are constants. The Tait equation of state provides a reasonable representation of the volumetric response of soft tissues embedded in a fluid medium and was, therefore, employed to describe the pressure response of all the head structures except the skull. To obtain the necessary parameters, Γ_0 was taken to be the value for water ~ 6.15. Appropriate bulk modulus values K were selected from the literature, and B was computed for each structure from Γ_0 and K using the relation:

$$K_0 = B \times (\Gamma_0 + 1) \tag{5}$$

Table 2 contains the parameters for the Tait equation of state used in the simulations.

Deviatoric elasticity

As mentioned above, an important component of a stress wave propagating in solid materials is the shear wave. This may be particularly important in the case of the response of brain tissue to blast as it causes transverse or shear strains and potential damage to axons. In addition, the shear wave effects may be exacerbated by tissue anisotropy and thus, increase the potential for injury. This is particularly true in the white matter where the fascicular directionality of the fiber bundles is likely to increase tissue vulnerability to shear stresses.

In order to describe the shear wave component, the model needs to account for the deviatoric response. Toward this end, an elastic deviatoric model was combined with the volumetric equation of state following a stress-strain relation of the following form (Cuitiño, 1992; Holzapfel, 2001; Ortiz, 1999):

$$\sigma^B = -PI + J^{-1} F^e \left[\mu \left(\log \sqrt{C^e} \right)^{dev} \right] F^{eT} \tag{6}$$

where $\boldsymbol{C}^e = \boldsymbol{F}^{eT}\boldsymbol{F}^e$ is the elastic Cauchy-Green deformation tensor, $log\sqrt{\boldsymbol{C}^e}$ is the logarithmic elastic strain, μ is a shear modulus, and the pressure P follows from the equations of state defined in Equations (2) and (4). Explicit formulae for the calculation of the exponential and logarithmic mappings, and the calculation of their first and second linearizations, have been given by Ortiz et al.(Ortiz, 2001) For the blast and impact simulations, values of μ were selected from the literature (Table 2).

The two blast fluid-solid interaction simulations were run on 20 processors, 14 of

which were assigned to the solid solver and 6 to the fluid. This proved sufficient to obtain the results in a reasonable time. Two levels of grid subdivision were employed in the fluid to resolve the blast front and the fluid-solid interface with enough fidelity. In the simulations, the lower region of the head was fixed where the neck would ordinarily be attached to the head in order to avoid the blast engulfing the bottom of the head. The solid-only impact simulation was run on 20 processors.

Results

5.2 atm Simulation

Figures 2(a) to 2(e) illustrate the propagation of the compressive blast wave through the coronal sections of the head in the 5.2 atm simulation. The blast wave is incident on the right temporal region (radiological convention). The compressive wave is seen propagating through the cranial cavity from the right to the left with some minor reflection from the left side of the cavity, leading to a pocket of concentrated pressure in the skull on the right-hand side of the head. In the coronal plane pressure amplitude - time curves at individual nodes in differing tissue regions are illustrated in Figure 3. This shows differential and decremental tissue responses depending on the location with the potential for significant differential strain even without the development of transverse or shear waves. Similar effects are seen in the sagittal plane as illustrated in Figure 4 (a) and 4 (b).

The maximum tensile and compressive pressures and Von Mises stress for the entire head were then extracted for each time step and plotted. These curves, which are

the envelopes of the pressure and stress histories of all points within the head, are given in Figures 5(a) to 5(f) for blast and impact simulations. The maximum tensile and compressive pressures were then extracted and plotted for each time step for each of the 11 distinct structures. These curves are shown in Figures 6(a) and 6(f) Overall, the maximum compressive pressure reached was 6.5 MPa at .00045 s, the maximum tensile pressure reached was .89 MPa at .00048 s. The maximum impact stresses appeared to develop with a more monotonic quality. The highest compressive pressures were experienced by the skull and muscle, followed by the subarachnoid CSF. The skull experienced higher stresses due to its more rigid (higher stiffness) material properties. The structures can be crudely divided into two groups: muscle, skull, CSF, gray matter, skin/fat, and air sinuses all experienced high compressive pressure, while the venous sinuses, ventricle, glia, white matter, and eyes tissue experienced a differing time course and a lower intensity. The different structures also experienced peak compressive pressure at different times, with gray matter intermediate, between the muscle, skull, CSF, and skin/fat. The structures that experienced the highest tensile pressure were sinus, gray matter, CSF, skull, and white matter. In this simulation, the nodes that experienced the highest pressures and stresses were all located on the right side of the head, in the concentrated pocket of stress created by the reflection of the blast wave from the left-side of the head.

18.6 atm Simulation

At the LD_{50} blast wave overpressures of ~ 18.6 atm, the compressive wave propagation is seen in Figure 7. Differential stresses are generated as the wave

propagates through the brain tissue. Wave reflection is more apparent at this overpressure as seen by the multiphasic pressure curves compared to Figure 5 and 6. Similar coronal and sagittal reconstructions at selected nodes are seen in Figures 8 and 9. The 18.6 atm simulation reached a maximum compressive pressure of 39 MPa at .00042 s in the skull and muscle, a maximum tensile pressure of 4.5 MPa at .00041 s in the gray matter area. High compressive pressures were experienced by the skull, muscle, CSF, gray matter, and skin/fat material elements. The skull peaked first, then the CSF and muscle and finally the gray matter. In the case of the tensile pressure, the highest pressure values were experienced by the skull, CSF, and gray matter followed by the white matter. Compared to the 5.2 atm simulation the 18.6 atm simulation generated pressures that were 4-6 times higher than those at 5.2 atm. Further the pressures and stresses also peaked earlier in the 18.6 atm simulation. However the locations in the head that experienced the highest stresses were very similar in both the 5.2 atm and 18.6 atm simulations.

Impact Simulation

The 5 m/s impact simulation ran to .000634 s, reaching a maximum compressive pressure of 27.2 MPa, a maximum tensile pressure of 7.1 MPa. The impact was delivered in the mid-coronal plane in a lateral direction, from left to right (Figures 10 – 12). Significant differences are seen between blast and impact injury specifically in the monotonic form of the impact compression and tension curves. The highest compressive pressures were also found in the skull, CSF, muscle, skin/fat and the gray matter with the highest compressive pressure being experienced by the skull itself. High tensile pressures

were experienced by the skull, muscle, skin/fat, and gray matter, with the highest tensile pressures again being experienced by the skull. The magnitudes of the maximum pressures reached in the impact simulation are comparable to the maximum pressures reached in the 18.6 atm simulation. This suggests that blasts that would result in 50% lethality due to unarmored parenchymal lung injury would lead to concussive injury in the brain since the impact simulation was based on the known parameters for sports concussive injury.(Casson, 2008)

Discussion

The use of personal protective equipment (PPE), particularly body armor, is considered to be protective against lethal blast and fragmentation lung injury. The goal of this work was to use the standardized Bowen curves for threshold and 50% lethal lung injury to examine and compare the effects of similar currently survivable blast exposure on the head. This was then subsequently compared with impact decelerations brain injury often seen within sports concussions such as in the National Football League.(Casson, 2008; Zhang, 2004) The analysis indicated that a blast consistent with lung $LD_{50\%}$ i.e. a blast in the pre-PPE era that would result in 50% lethality from lung injury would also be associated with a concussion equivalent to impact injury that may result from a sports concussion or mild TBI (mTBI).

From the model it is observed that direct propagation of blast waves into the brain occurs confirming one of the original stated hypotheses. Further with exposure to the

equivalent of 0.324 kg TNT at a 0.6 m standoff distance (18.6 atm overpressure), a similar order of magnitude stress develops within CNS tissues comparable to those known to be significant in the development of sport concussive injury or mTBI. The American Academy of Neurology grades sports concussion from grade 1 – 3. Only grade 3 indicates a loss of consciousness while grade 1 and 2 represent transient confusion or loss of situational awareness.(Quality Standards Committee of the American Academy of Neurology, 1997) In the military context such transient confusion or loss of situational awareness within a combat environment may slow reaction and response time to adverse events with potentially devastating results.

The blast-solid interaction simulation technology employed in this work is well established and has been validated in the case of the response of engineering materials such as steel and aluminium plates.(Cummings, 2002; Kambouchev, 2007a) Also, for the case of impact conditions in which blast is not involved, there have been efforts to validate this type of simulations (Zhang, 2004). Although there are currently no validated models for the case of blast effects on the human head, there are current efforts focusing on the experimental test programs using animal models that will be used for model validation in extension of the present work. This ongoing work will combine field blast tests and a porcine full head model simulation. The blast events will be monitored using external pressure sensors together with animal instrumentation. The number of internal and external pressure experimental sensors will necessarily be limited and will fall far short of the theoretical number of sensors required to completely and uniquely capture the complex 3-D fluid flow field associated with a blast. This crucially emphasizes the

importance and value of simulation work where the complete dataset is available for interrogation. Both approaches, the field investigational and the numerical/computational must be regarded as complementary in enhancing understanding of these complex fluid-solid interaction blast events in biological tissue such as the CNS.

The constitutive model and properties used in the current blast simulations will be refined as experimental tissue response characterization results become available at blast-relevant strain rates. However, the models and properties used represent "good first order approximations" that are extrapolated from impact conditions into the blast strain-rate domain. The three contexts compared in this paper are: (a) a peak blast over pressure of 5.2 atm equivalent to free air explosion of 0.0648 kg TNT at 0.6 m stand-off and corresponding to the Bowen threshold for un-armored lung parenchymal injury (b) a peak blast over pressure of 18.6 atm equivalent to free air explosion of 0.324 kg TNT at 0.6 m stand-off and corresponding to the Bowen 50% lethality for un-armored lung parenchymal injury and (c) impact deceleration of the full head model from a velocity of 5 m/s to 0 m/s following impact with a stationary immovable boundary. While other comparative combinations could have been considered, these specifically provide calculable evidence for concussive brain injury following primary blast exposure at a specific standoff and TNT equivalence. The results indicate a potential for concussive effects from blast under the strict model conditions applied. This suggests, at a minimum that such a potential threat deserves further considered investigation and consideration. CNS stress waves may also be generated by ballistic injury and the effect of a stress wave

generated by ballistic impact conditions and TBI have been recently discussed.(Courtney, 2007)

Blast associated TBI is probably rarely isolated or primary but more likely to be combined with secondary shrapnel or fragment injury, or tertiary blast injury due to impact such as occurs with vehicle roll-over or hitting a stationary wall.(Warden et al., 2009) The biological independent and synergistic effects of detonation products on brain injury cannot be excluded and is part ongoing scientific investigation.(Moore, 2008) The model described in this paper can also be used to explore such multi-physics effects. Other areas of current investigation are examination of the relative contribution of direct pressure effects and indirect transmission of pressure effects on the brain through the great vessels.(Cernak et al., 1999; Moore, 2008)

It is hoped that a direct applications of the modeling presented in this paper will be to shorten the design cycle of engineering modifications for the development of personal protective equipment. Currently head PPE tends to be optimized for impact or ballistic protection with little or no consideration of blast mitigation or protection. The complexity of issues required to consider in engineering optimization of head PPE should not be underestimated and may further represent an avenue where models such as the one developed in the current work could substantially contribute.

Conflict of Interest Statement

The authors have no conflicts of interest to disclose.

Acknowledgements

This work was support in full by financial aid from the Joint Improvised Explosive Device Defeat Organization (JIEDDO) through the Army Research Office. We also thank the Editorial Staff of NeuroImage for the helpful critique and comment on this manuscript.

Legends for Submitted Supplementary Movies

Movie 1. DVBIC – MIT full head model (FHM) associated with the advanced combat helmet (ACH) and standard helmet pad configuration PPE. The frames show the rendered finite element (FE) meshes followed by the unstructured mesh geometry for each component of the FHM.

Movie 2. The DVBIC – MIT full head model cut in the mid-sagittal plane showing the transmission and propagation of a tensile wave through the CNS. It is seen that a preferential pathway of wave propagation appears to concentrate in the white matter areas.

References

Quality Standards Committee of the American Academy of Neurology, 1997. Practice Parameter: The Management of Concussion in Sports. Neurology 48, 581 - 585.
Bass, C., et al., 2006. Pulmonary injury risk assessment for short-duration blasts. Proceedings of the Personal Armour Systems Symposium (PASS), Leeds, UK.
Belingardi, G., Chiandussi, G, Gaviglio, I, 2005. Development and validation of a new finite element model of human head. 19th International Technical Conference on the Enhanced Safety of Vehicles Conference, Washington, D.C.

Bowen, I., Fletcher, ER, Richmond, DR, Hirsch, FG, White, CS, 1968. Biophysical mechanisms and scaling procedures applicable in assessing responses of the thorax energized by air-blast overpressures or by nonpenetrating missiles. Ann N Y Acad Sci 152, 122 - 146.
Brands, D., Peters, GWM, Bovendeerd, PHM, 2004. Design and numerical implementation of a 3-D non-linear viscoelastic constitutive model for brain tissue during impact.. Journal of Biomechanics 37, 127 - 134.
Brazarian, J., McClung, J, Shah, M, Cheng, Y, Flesher, W, Kraus, J, 2005. Mild traumatic brain injury in the United States. Brain Injury 18, 85 - 91.
Bruns, J., Hauser, AW, 2003. The epidemiology of traumatic brain injury: a review. Epilepsia 44, 2 - 10.
Casson, I., Pellman, EJ, Viano, DC, 2008. Concussion in the national football league: an overview for neurologists. Neurol Clin 26, 217 - 241.
Cernak, I., Savic, J., Ignjatovic, D., Jevtic, M., 1999. Blast injury from explosive munitions. J Trauma 47, 96-103; discussion 103-104.
Coats, B., Margulies, SS, 2006. Material properties. Biomechanics 39, 2521 - 2525.
Collins, D., Zijdenbos, AP, Kollokian, V, et al, 1998. Design and construction of a realistic digital brain phantom. IEEE Trans Med Imaging. 1998;17:463 - 469 17, 463 - 469.
Courtney, A., Courtney, M, 2007. Links between traumatic brain injury and ballistic pressure waves originating in the thoracic cavity and extremities. Brain Injury 21.
Cuitiño, A., Ortiz, M, 1992. A material-independent method for extending stress update algorithms from small-strain plasticity to finite plasticity with multiplicative kinematics. Engineering Computations 9, 437 - 451.
Cullis, I., 2001. Blast waves and how they interact with structures. J R Army Med Corps 147, 18 - 26.
Cummings, J., Aivazis, M, Samtaney, R, Radovitzky, R, Mauch, S, D. Meiron, D, 2002. A virtual test facility for the simulation of dynamic response in materials. J. Supercomput 23, 39 - 50.
Deiterding, R., Radovitzky, R, Mauch, SP, Noels, L, Cummings, JC, Meiron, I, 2006. A virtual test facility for the efficient simulation of solid material response under strong shock and detonation wave loading. Engineering with Computers 22, 325 - 244.
DePalma, R., Burris, DG, Champion, HR, Hodgson, MJ, 2005. Blast Injury. N Eng J Med 353, 1335 - 1342.
Drapaca, C., Tenti, G, Rohlf, K, Sivaloganathan, S, 2006. A quasi-linear viscoelastic constitutive equation for the brain: application to hydrocephalus. Journal of Elasticity 85, 65 - 83.
Drumheller, D., 1998. Introduction to wave propagation in nonlinear fluids and solids. Cambridge University Press, Cambridge.
Elsayed, N., 1997. Toxicology of blast overpressure. Toxicology 121, 1 - 15.
Gefen, A., Margulies, SS, 2004. Are in vivo and in situ brain tissues mechanically similar? Journal of Biomechanics 37, 1339 - 1352.
Gilchrist, M., O'Donoghue, D, Horgan, T, 2001. Gilchrist MD, O'Donoghue, D, Horgan, T. A two-dimensional analysis of the biomechanics of frontal and occipital head impact injuries. Int. J. Crashworthiness. 2001;6:253-262.

Holzapfel, G.A., 2001. Nonlinear solid mechanics: a continuum approach for engineering. John Wiley & Sons Ltd, Chichester, England.
Horgan, T., Gilchrist, MD, 2004. Influence of FE model variability in predicting brain motion and intracranial pressure changes in head impact simulations. Int. J. Crashworthiness 9, 401 - 418.
Iverson, G., Lange, RT, Gaetz, M, Zasler, ND, 2006. Mild TBI. In: Zasler, N., Katz, DI, Zafonte, RD (Ed.), Brain Injury Medicine. Demos, New York.
Kambouchev, N., Noels, L, Radovitzky, R, 2006. Nonlinear compressibility effects in fluid-structure interaction and their implications on the air-blast loading of structures. Journal of Applied Physics 100, 063519 - 063511.
Kambouchev, N., Noels, L, Radovitzky, R, 2007a. Numerical simulation of the fluid-structure interaction between air blast waves and free-standing plates. Computers and Structures 23, 325 - 347.
Kambouchev, N., Radovitzky, R, Noels, L, 2007b. Fluid–Structure Interaction Effects in the Dynamic Response of Free-Standing Plates to Uniform Shock Loading. Journal of Applied Mechanics 74, 1 - 5.
Kolsky, H., 1963. Stress Waves in Solids. Dover Publications, New York.
LaPlaca, M., Cullen, DK, McLoughlin, JJ, Cargill II, RS, 2005. High rate shear strain of three-dimensional neural cell cultures: a new in vitro traumatic brain injury model. Journal of Biomechanics 38, 1093 - 1105.
Mayorga, M.A., 1997. The pathology of primary blast overpressure injury. Toxicology 121, 17-28.
Meyers, M., 1994. Dynamic behavior of materials. Wiley Interscience, New York.
Miller, K., 1999. Constitutive model of brain tissue suitable for finite element analysis. Journal of Biomechanics 32, 531 - 537.
Miller, K., 2005. Method of testing very soft biological tissues in compression. Journal of Biomechanics 38, 153 - 158.
Miller, K., Chinzei, K, 2002. Mechanical properties of brain tissue in tension. Journal of Biomechanics 35, 483 - 490.
Moore, D., Radovitzky, RA, Shupenko, L, Klinoff, A, Jaffee, MS, Rosen, JM, 2008. Blast physics and central nervous system injury. Future Neurology 3, 243 - 250.
Morrison, B., Cater, HL, Benham, CD, Sundstrom, LE, 2006. An in vitro model of traumatic brain injury utilising two-dimensional stretch of organotypic hippocampal slice cultures. Journal of Neuroscience Methods 150, 192 - 201.
Ortiz, M., Radovitzky, RA, Repetto, EA, 2001. The computation of the exponential and logarithmic mappings and their first and second linearizations. International Journal for Numerical Methods in Engineering 52, 1431 - 1441.
Ortiz, M., Stainier, L, 1999. The variational formulation of viscoplastic constitutive updates. Computer Methods In Applied Mechanics And Engineering 171, 419 - 444.
Petras, J., Bauman, RA, Elsayed, NM, 1997. Visual system degeneration induced by blast overpressure. Toxicology 121, 41 - 49.
Prange, M., Margulies, SS, 2002. Regional, directional, and age-dependent properties of the brain undergoing large deformation. Journal of Biomechanical Engineering 124, 244 - 252.

Raul, J., Baumgartner, D, Willinger, R, Ludes, B, 2006. Finite element modelling of human head injuries caused by a fall International Journal of Legal Medicine 120, 212 - 218.
Saraf, H., Ramesh, KT, Lennon, AM, Merkle, AC, Roberts, IC, 2007. Mechanical properties of soft human tissues under dynamic loading. Journal of Biomechanics 40, 1960 - 1967.
Shen, F., Tay, TE, Li JZ, Nigen, S, 2005. Modified Bilston nonlinear viscoelastic model for finite element head injury studies. Journal of Biomechanical Engineering 128, 797 - 801.
Strehlow, R., Baker, WE, 1976. The characterization and evaluation of accidental explosions. Progress in Energy and Combustion Science 2, 27 - 60.
Stuhmiller, J., 1987. Biological response to blast overpressure: A summary of modeling. Toxicology 121, 91 - 103.
Tanielian, T., L, 2008. Invisible wounds of war: psychological and cognitive injuries, their consequences, and services to assist recovery. In: Tanielian, T., Jaycox, LH (Ed.). RAND Corporation, Center for Military Health Policy Research, Santa Monica, CA.
Taylor, P., Ford, CC, 2006. Simulation of head impact leading to traumatic brain injury Army Science Conference Orlando, FL.
Velardi, F., Fraternali, F, Angelillo, M, 2006. Anisotropic constitutive equations and experimental tensile behavior of brain tissue. Biomech. Model Mechanbiol 5, 53 - 61.
Warden, D., French, LM, Shupenko, L, Fargus, J, Riedy, G, Erickson, ME, Jaffee, , MS, M., DF, 2009. Case Report of a Soldier with Primary Blast Brain Injury. Neuroimage In Press.
White, C., Jones, RK, Damon, EG, Fletcher, ER, Richmond, DR, 1971. The biodynamics of airblast. In: Defense Nuclear Agency, T.R. (Ed.), Washington, D.C.
Willinger, R., Baumgartner, D, 2003. Numerical and physical modelling of the human head under impact - towards new injury criteria. Int. J. Vehicle Design 32, 94 - 115.
Zel'dovich, T., Raizer, YP, 1967. Physics of shock waves and high-temperature hydrodynamic phenomena. Academic Press, New York.
Zhang, L., Yang, KH, Dwarampudi, R, Omori, K, Li, T, Chang, K, Hardy, WN, , Khalil, T., King AI, 2001. Recent advances in brain injury research: a new human head model development and validation. Stapp Car Crash Journal 45, 369 - 394.
Zhang, L., Yang, KH, King, AI, 2004. A proposed injury threshold for mild traumatic brain injury. Journal Biomechanical Engineering 126, 226 - 236.

Structure	*$\rho(kg/m^3)$*	*E(Pa)*	*ν*	*C_0*	*S*
Skull	1412	6.5e9	0.22	1.85e3	0.94

Table 1: Parameters for the Mie-Gruneisen/Hugoniot Equation of State

Structure	*ρ*	*K(Pa)*	*B*	*Γ_0*	*μ(Pa)*
Ventricle	*1040*	*2.19e9*	*3.063e8*	*6.15*	*2.25e4*
Glia	*1040*	*2.19e9*	*3.063e8*	*6.15*	*2.253e4*
White Matter	*1040*	*2.19e9*	*3.063e8*	*6.15*	*2.253e4*
Gray Matter	*1040*	*2.19e9*	*3.063e8*	*6.15*	*2.253e4*
Eyes	*1040*	*2.19e9*	*3.063e8*	*6.15*	*2.253e4*
Venous Sinus	*1040*	*2.19e9*	*3.063e8*	*6.15*	*2.013e4*
CSF	*1040*	*2.19e9*	*3.063e8*	*6.15*	*2.253e4*
Air Sinus	*1040*	*2.19e9*	*3.063e8*	*6.15*	*2.253e2*
Muscle	*1100*	*3.33e6*	*4.662e5*	*6.15*	*3.793e4*
Skin/Fat	*1040*	*3.47e7*	*4.866e6*	*6.15*	*5.880e6*

Table 2: Parameters for the Tait Equation of State

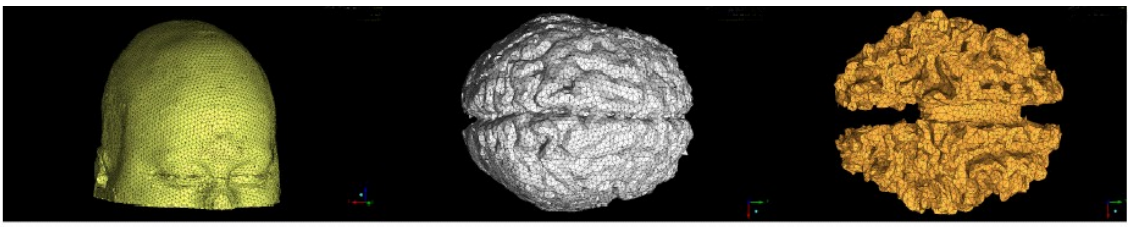

(a) (b) (c)

Fig. 1: DVBIC – MIT full head finite element model showing progressively more internal tissue layers. The skin (figure 1(a)), gray matter (figure 1(b)), and white matter (figure 1(c)) from the 808,766-element head mesh used in the fluid – solid interface blast simulations.

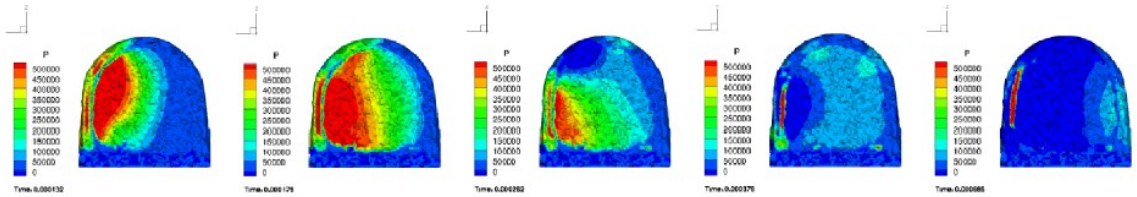

(a) .132 ms **(b).178 ms** **(c) .262 ms** **(d) .376 ms** **(e) .685 ms**

Figure 2. Propagation of blast compressive wave through cranial cavity in 5.2 atm simulation, viewed through mid-coronal plane at 0.132 – 0.685 ms. The propagation of the blast wave is from left to right in the external observer frame of reference. Scale is from 0 to 500 kPa.

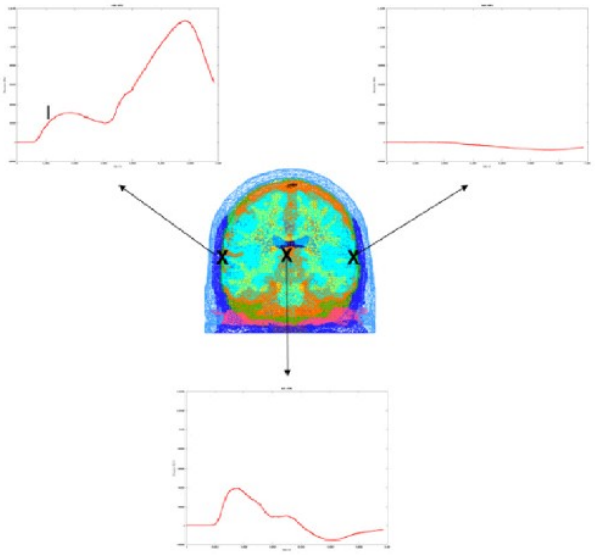

Figure 3: Pressure histories of selected nodes in the mid-coronal plane. Clockwise from top left, the nodes are located in the skull, skull and gray matter. The scale is from -0.2 to 1.4 MPa.

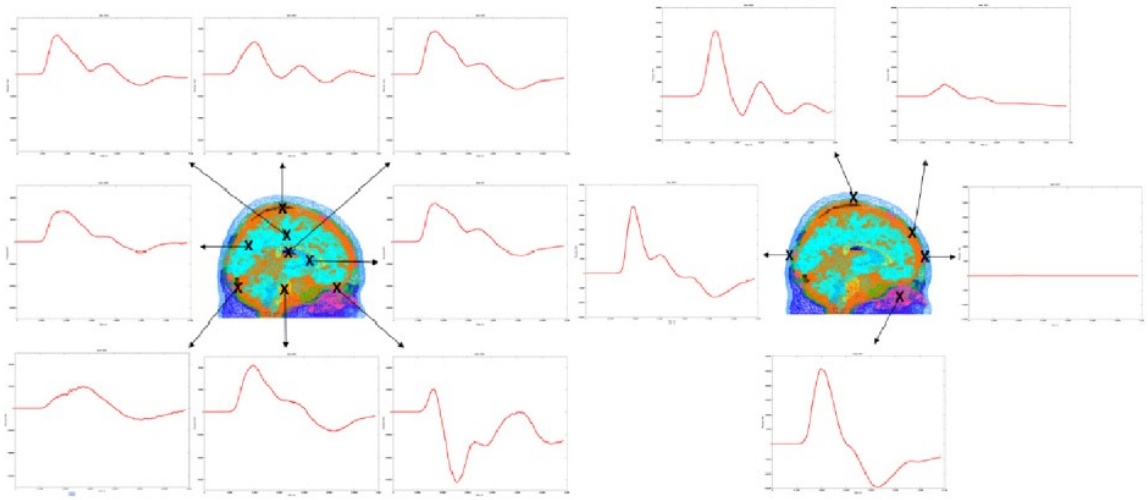

(a) (b)

Figure 4. Pressure histories of selected nodes in the mid-sagittal plane. Fig. 4(a) shows the pressure histories of nodes within the cranial cavity. Clockwise from top right, the nodes are located in the glia, ventricles, csf, white matter, csf, gray matter, gray matter, and venous sinuses. The scale is from -700 to 500 kPa. Fig. 4(b) shows the pressure histories of nodes on or outside the cranial cavity. Clockwise from top right, the nodes are located in the skull, skull, air sinuses, skin/fat, and skull. The scale is from -150 to 300 kPa.

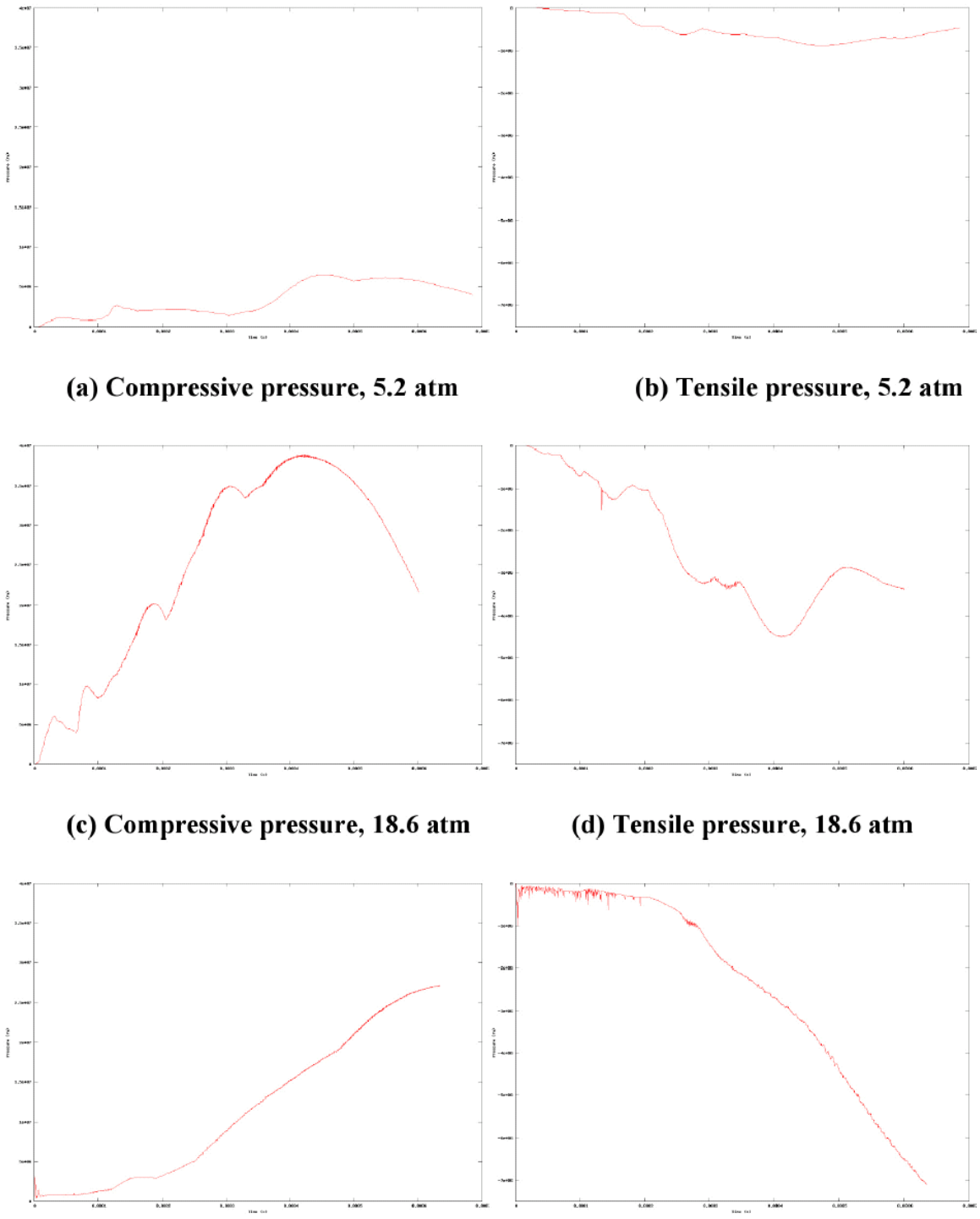

(a) Compressive pressure, 5.2 atm **(b) Tensile pressure, 5.2 atm**

(c) Compressive pressure, 18.6 atm **(d) Tensile pressure, 18.6 atm**

(e) Compressive pressure, 5 m/s impact **(f) Tensile pressure, 5 m/s impact**

Figure 5. Maximum overall compressive and tensile pressures for 5.2 atm, 18.6 atm, and 5 m/s impact simulations.

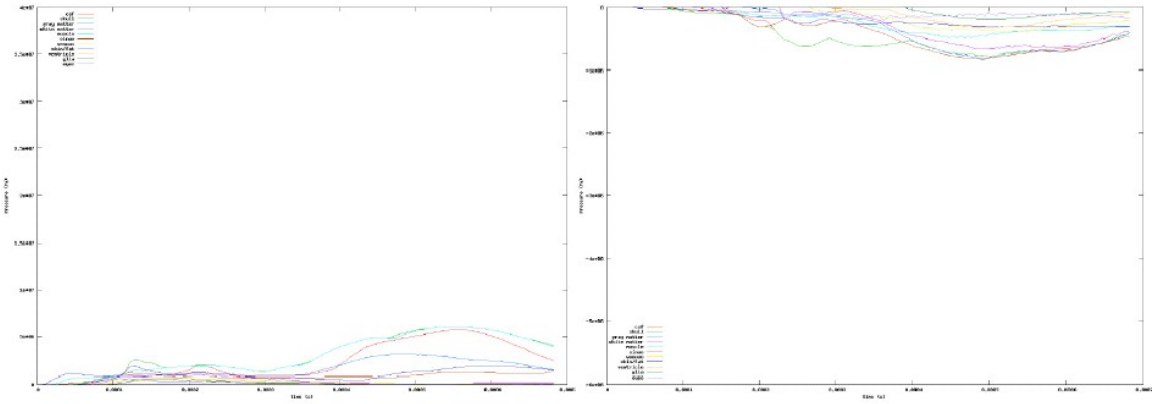

(a) Compressive pressure, 5.2 atm (b) Tensile pressure, 5.2 atm

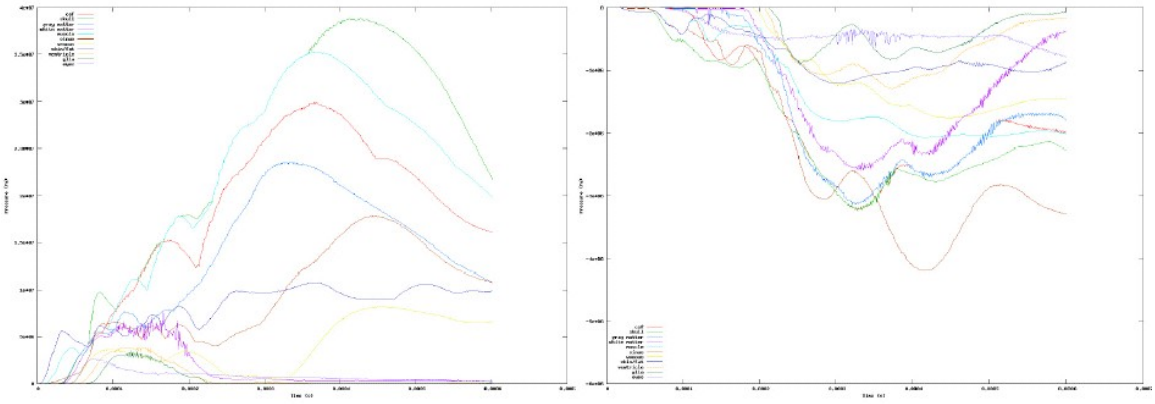

(c) Compressive pressure, 18.6 atm (d) Tensile pressure, 18.6 atm

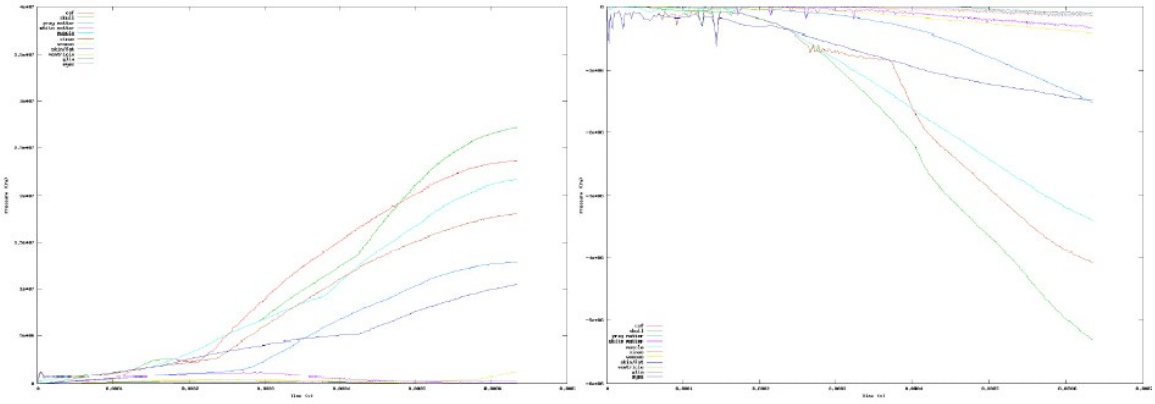

(e) Compressive pressure, 5 m/s impact (f) Tensile pressure, 5 m/s impact

Figure 6. Maximum compressive and tensile pressures reached by differentiated structures in 5.2 atm, 18.6 atm, and 5 m/s impact simulations.

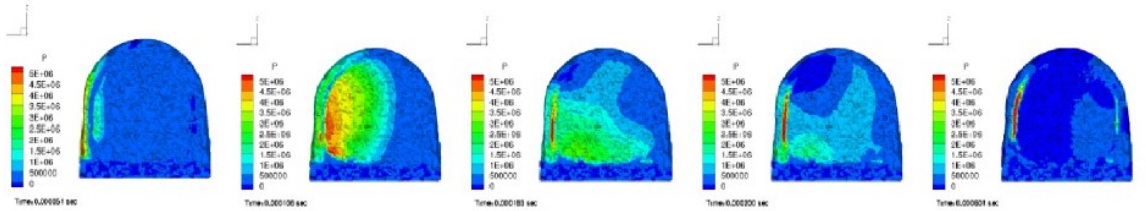

(a) .051 ms **(b) .108 ms** **(c) .183 ms** **(d) .200 ms** **(e) .601 ms**

Figure 7. Propagation of compressive wave through cranial cavity in 18.6 atm simulation, viewed through mid-coronal plane over a time range of 0.051 – 0.601 ms. Blast wave is propagated from left to right in the external frame of reference. Scale is from 0 to 5 MPa.

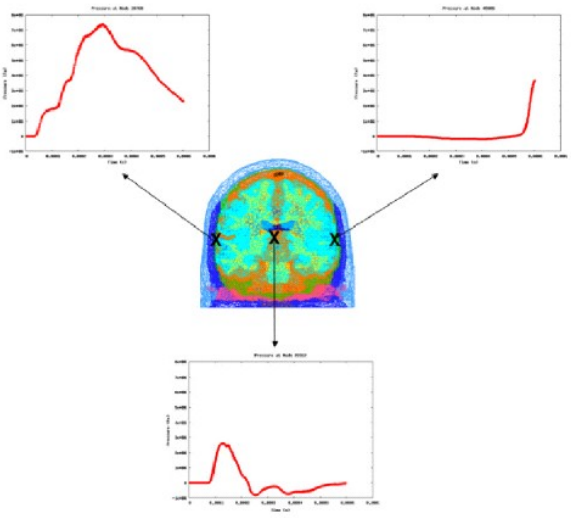

Figure 8. Pressure histories of selected nodes in the mid-coronal plane. The scale is from -1 MPa to 8 MPa.

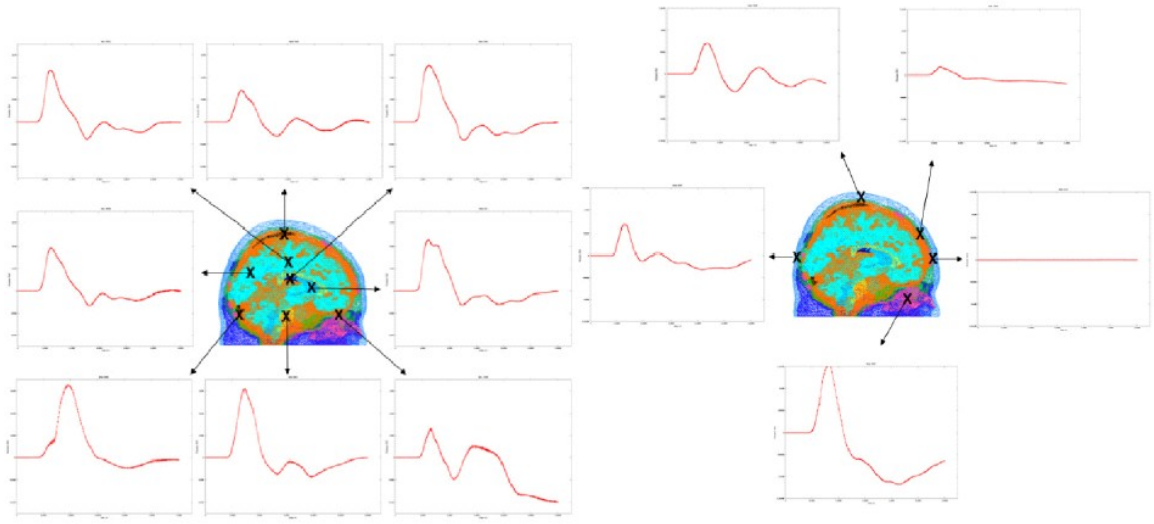

(a) (b)

Figure 9. Pressure histories of selected nodes in the mid-sagittal plane. In Fig. 9(a), the scale is from -2.5 MPa to 3.5 MPa. In Fig. 9(b), the scale is from -1.5 MPa to 1.5 MPa.

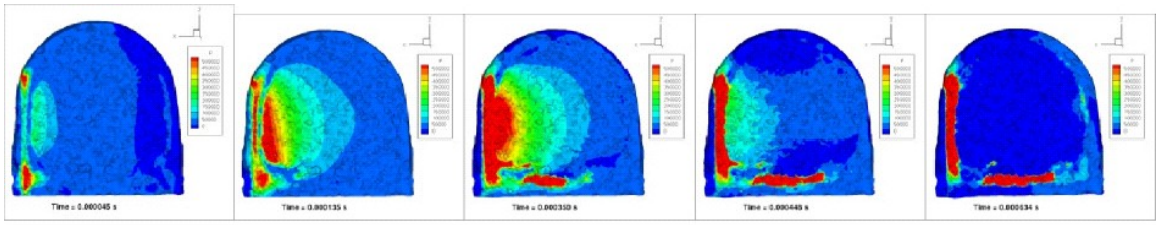

(a) .045 ms **(b) .135 ms** **(c) .350 ms** **(d) .448 ms** **(e) .634 ms**

Figure 10. Propagation of compressive wave through cranial cavity in 5 m/s impact simulation, viewed through mid-coronal plane.

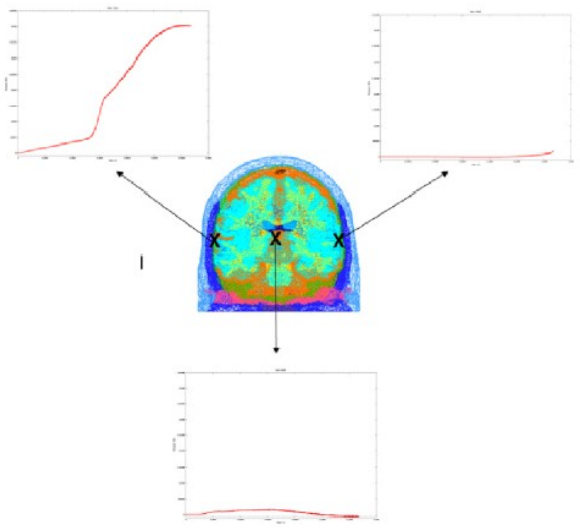

Figure 11. Pressure histories of selected nodes in the mid-coronal plane. Scale is from -100 kPa to 4.5 MPa.

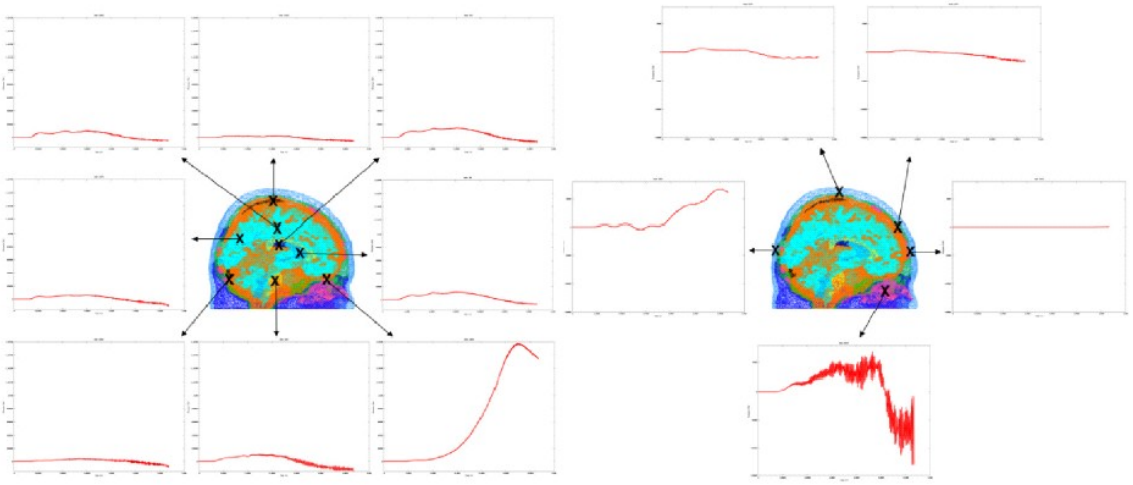

Figure 12. Pressure histories of selected nodes in the mid-sagittal plane. In fig. 12(a), the scale is from -150 kPa to 1.8 MPa. In Fig. 12(b), the scale is from -150 kPa to 80 kPa.